AD-A240 023

||||||||||||

REPORT NO. T13-91

A COMPUTER SIMULATION FOR PREDICTING THE TIME COURSE OF THERMAL AND CARDIOVASCULAR RESPONSES TO VARIOUS COMBINATIONS OF HEAT STRESS, CLOTHING AND EXERCISE

U S ARMY RESEARCH INSTITUTE

OF

ENVIRONMENTAL MEDICINE

Natick, Massachusetts

JUNE 1991

DTIC
ELECTE
SEP. 0 4 1991
S
B
D

91-09526
||||||||||||

UNITED STATES ARMY
MEDICAL RESEARCH & DEVELOPMENT COMMAND

9: (4 021

The findings in this report are not to be construed as an official Department of the Army position, unless so designated by other authorized documents.

DISPOSITION INSTRUCTIONS

Destroy this report when no longer needed.

Do not return to the originator.

REPORT DOCUMENTATION PAGE			Form Approved OMB No 0704-0188

1. AGENCY USE ONLY (Leave blank)	2. REPORT DATE June 1991	3 REPORT TYPE AND DATES COVERED Technical Report

4. TITLE AND SUBTITLE	5. FUNDING NUMBERS
A Computer Simulation for Predicting the Time Course of Thermal and Cardiovascular Responses to Various Combinations of Heat Stress, Clothing and Exercise	

6. AUTHOR(S)

Kenneth K. Kraning II

7. PERFORMING ORGANIZATION NAME(S) AND ADDRESS(ES)	8. PERFORMING ORGANIZATION REPORT NUMBER
U.S. Army Research Institute of Environmental Medicine Natick, MA 01760-5007	

9. SPONSORING/MONITORING AGENCY NAME(S) AND ADDRESS(ES)	10. SPONSORING/MONITORING AGENCY REPORT NUMBER
Same as 7.	

11. SUPPLEMENTARY NOTES

12a. DISTRIBUTION/AVAILABILITY STATEMENT	12b DISTRIBUTION CODE
Approved for public release; distribution is unlimited.	

13. ABSTRACT (Maximum 200 words)

This report describes a new computer simulation of human temperature regulation for predicting limiting physiological responses to work under heat stress. Possible military applications include adjustment of work:rest cycles during intermittent work in protective clothing or confined spaces and determining optimal recovery periods and environments following exercise and/or exposure to hot environments. Using a database from 7 independent studies of widely varying workload and environment, the simulation was validated by comparing the standard deviations (sd) of variable means (internal temperature, skin temperature and heart rate) in the data sets with the root mean squared deviations (rmsd) between the variable means and the corresponding simulator outputs. Results suggest that, on the average and within the range of data tested, the present simulation is able to forecast results with the same order of precision as laboratory studies of the same problems. Future applications could include incorporation into on-line expert systems used as tactical decision aids and as a tool to aid the experimental design of studies on the competing stresses of work, heat, dehydration, sleep deprivation and chemical protective drugs.

14. SUBJECT TERMS			15. NUMBER OF PAGES 52
mathematical models; human temperature regulation; regional blood flow; cardiac stroke volume control; skin thermal conductance			16. PRICE CODE

17. SECURITY CLASSIFICATION OF REPORT	18. SECURITY CLASSIFICATION OF THIS PAGE	19. SECURITY CLASSIFICATION OF ABSTRACT	20. LIMITATION OF ABSTRACT
UNCLASSIFIED	UNCLASSIFIED	UNCLASSIFIED	

TECHNICAL REPORT

NO. T13-91

A COMPUTER SIMULATION FOR PREDICTING THE TIME COURSE OF THERMAL AND CARDIOVASCULAR RESPONSES TO VARIOUS COMBINATIONS OF HEAT STRESS, CLOTHING AND EXERCISE

by

Kenneth K. Kraning II

June 1991

U. S. Army Research Institute of Environmental Medicine
Natick, Massachusetts 01760-5007

DISCLAIMER

The views, opinions and/or findings in this report are those of the authors, and should not be construed ~ an official Department of the Army position, policy or decision, unless so designated by . ther official documentation.

Citations of commercial organizations and trade names in this report do not constitute an official Department of the Army endorsement or approval of the products or services of these organizations.

Approved for public release; distribution is unlimited.

Accession For	
NTIS GRA&I	☑
DTIC TAB	☐
Unannounced	☐
Justification	
By	
Distribution/	
Availability Codes	
Dist	Avail and/or Special
A-1	

CONTENTS

ACKNOWLEDGEMENTS

EXECUTIVE SUMMARY

This report describes a computer simulation of human temperature regulation for predicting important physiological responses during exercise and exposure to heat stress. Although the construct is similar to existing thermoregulatory simulations, several novel features have been formulated. First, the skin is not modeled as a single compartment but as two compartments corresponding to the deep vascular and the superficial avascular layers. Second, new algorithms are used to control regional blood flow to skin, to muscle and to core (viscera and other internal organs). Third, a new algorithm that modulates conductance between the vascular and avascular skin layers. Fourth, there is a new model of the central circulation that controls cardiac stroke volume and restrains blood flow to muscle and to skin when demands exceed the maximal cardiac output. Finally, the complexity of the passive system is tailored to match the problem of exercise in hot environments where internal and surface body temperature gradients are relatively small, symmetrical and change slowly. Using a database from 7 independent studies of widely varying workload and environment, the simulation was validated by comparing the standard deviations (sd) of variable means (internal temperature, skin temperature and heart rate) in the data sets with the root mean squared deviations (rmsd) between the variable means and the corresponding simulator outputs. Except for skin temperature, for which there was some uncertainty about experimental conditions, the average sd and the average rmsd were similar in value: a difference of $\pm0.03°C$ for internal temperature, 0 beats•min^{-1} for heart rate and $\pm0.78°C$ for skin temperature. This variability suggests that, on the average and within the range of data tested, the present simulation is able to forecast results with the same order of precision as laboratory studies of the same problems. Possible military applications include the accurate prediction of heat strain and adjustment of work:rest cycles during intermittent work in protective clothing and in confined spaces and determination of optimal recovery periods following exercise and/or exposure to hot environments. A further application of the simulation could be to assist in the design of militarily relevant studies on the competing demands of work, heat, sleep deprivation and chemical protective agents.

1

2

Introduction

A computer simulation can serve as a vector for translating specific physiological knowledge into practical guidelines for solving real-world problems. Of particular military and industrial relevance would be a simulation of thermoregulation designed specifically to forecast temperature changes within the body, as well as cardiovascular and other physiological responses during work in the heat. Such a simulation would be a useful tactical decision aid for predicting the level of heat strain and casualty rates likely to arise from different scenarios of activity, environment and protective clothing and for optimizing personnel turnover rates and adjusting the time periods in work:rest cycles.

Computer simulations of thermoregulation typically incorporate sets of equations describing systems that are physically passive and physically active in heat transfer processes. The passive system defines the geometry of the body container space as one or more segments, divides the segments into one or more tissue compartments, and calculates temperature distributions and rates of heat transfer within compartments, segments and between the container and the environment. The active system defines the response of physiological control mechanisms that attempt to alter rates of heat transfer in the passive system in response to deviations in compartment temperatures from certain threshold levels (31). Passive and active systems interact in a closed-loop, proportional-type control system (16).

The purpose of this report is to describe an uncomplicated mathematical simulation of thermoregulation with passive and active systems specifically designed for predicting the time-course of critical physiological responses of exercising humans during heat stress. The following features of this simulation are unique: (a) the skin is modeled as two components: a vascular layer, where heat is exchanged with the blood, and a superficial avascular layer, where heat is exchanged with the environment; (b) new algorithms are incorporated for controlling blood flow to skin, to muscle and to core (viscera); (c) increased heat transfer efficiency accompanying cutaneous venodilation is modeled with an algorithm for controlling thermal conductance between the vascular and avascular skin layers; and (d) a new paradigm of the central circulation is proposed incorporating algorithms for controlling cardiac stroke volume, and for reducing regional blood flow when demands for total blood flow exceed maximal cardiac output. Some non-thermoregulatory influences of exercise on circulatory components of the active system

3

are also considered (18,26). The simulation is further evaluated in this report by comparing simulator outputs with data obtained from seven independent studies of exercise in disparate environments.

Methods

DEVELOPMENT OF THE SIMULATION

Simulations of thermoregulation are usually constructed with specific intentions and definite applications in mind. The structural complexity that must be built into the passive and active components of a simulation largely depends upon the problem under investigation (8,10,14,21,31,32). A successful simulation to predict body temperature responses in and around the thermal comfort zone has been devised as one-dimensional heat flow between only two physical subdivisions or compartments: a core and a shell (10). At the other extreme are simulations of cold water immersion or of asymmetrical heating and cooling during space flight which require heat flow in more than one dimension between highly subdivided passive systems because of large and rapidly changing temperature gradients across the tissues that may not be symmetric throughout the body (14, 21). The optimal passive system of a simulation to mimic work in hot environments lies somewhere in between these two. On the one hand, a human heat strain simulation can employ fairly simple mathematical forms without sacrificing much accuracy because, during exercise and environmental heat stress, tissue temperature gradients are relatively small, can be considered symmetrical, and change rather slowly (14, 32). On the other hand, for accurate and comprehensive prediction of responses to exercise under heat stress, a simulation must model the thermal and circulatory changes within several body compartments. This requires a rather complex active system and a passive system that is more highly structured than the core-shell model.

The Passive or Controlled System

4

The human body is modeled as a single segment: an upright cylinder consisting of five concentric annular compartments (core, muscle, fat, vascular skin, avascular skin) and an interconnecting central blood compartment (Figure 1). A one segment model of the passive system was chosen over a more anatomical representation because data on heat exchange coefficients, clothing insulation and water vapor permeability constants, and the bulk of temperature and circulatory data needed to validate the simulation regard the body as a single entity, not as multiple segments each with its own physiological effector responses and internal temperature distribution.
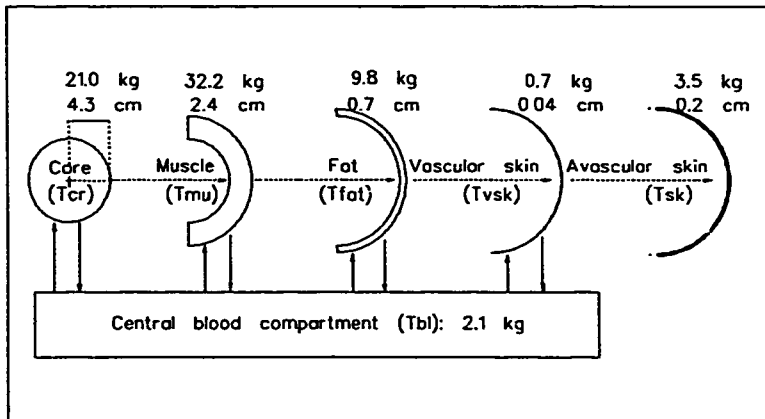

Figure 1. Cross-section of cylindrical model containing 5 concentric annular tissue compartments. Dimensions are for an individual with W = 70 kg, A_D = 1.8 m².

Within this upright cylinder, heat is conducted radially between adjacent annular compartments. There is no axial heat conduction and the cylinder ends are perfectly insulated. Each compartment is homogeneous and isotropic and, at any instant, of uniform temperature throughout. Intercompartmental resistance to heat flow occurs at a single imaginary concentric annular surface located midway between the centers of mass of adjacent compartments. Between the vascular and avascular skin layers conductance is controlled by the active system. Values for thermal conductance between other compartments are constant and vary only with the anthropometric characteristics of the particular subject.

5

Cylinder and compartment dimensions are computed from three anthropometric characteristics: body weight (W), stature (H) and percent of body weight that is fat (%fat). Overall body density (ρ), in $g \cdot cm^{-3}$, is estimated from the empirical relationship $\rho = (457)/(\%fat+412)$, as proposed by Brozek et al. (5). This formula assumes that the body is made up of only two components: fat ($\rho_{fat} = 0.9$) and nonfat ($\rho_{nfat} = 1.1$). V is calculated as W/ρ and the surface area (A_D), in cm^2, is given by the empirical DuBois formula (6): $A_D = (2020)(W)^{0.425}(H/100)^{0.725}$. The length of the cylinder (L) is obtained from the expression $(A_D)^2/(4\pi V)$, and the radius of the cylinder (r) from $(2V)/(A_D)$. The volume of the fat compartment (V_{fat}) is obtained from $(W)(\%fat)(\rho_{fat})$. The total volume of all non-fat compartments (V_{nfat}) is calculated as: $(W)(100 - \%fat)(\rho_{nfat})/(100)$. V_{nfat} is then distributed in the following way: 37% to core, 54% to muscle, 1% to vascular skin, 6% to skin and 2% to the central blood compartment (30).

The procedure for calculating compartment dimensions and thermal conductances within the passive system is similar to that described by Stolwijk and Hardy (30). Starting with the outermost avascular skin layer and $V_{out} = V$, the inner radius of each annular compartment is calculated in succession from the formula:

$$r_{in} = \sqrt{\frac{(V_{out} - V_{cmpt})}{\pi \cdot L}} \qquad [cm] \qquad (1)$$

The radii of concentric cylindrical surfaces located at the center of mass of each compartment are then obtained from:

$$r_{cm} = \sqrt{\frac{(V_{out} - 0.5 \cdot V_{cmpt})}{\pi \cdot L}} \qquad [cm] \qquad (2)$$

The radius and area of an imaginary concentric cylindrical surface lying at the midpoint between the centers of mass of adjacent compartments a and b are obtained from Equations 3 and 4, respectively:

$$r_{mp-ab} = \frac{r_{cm-a} - r_{cm-b}}{2} \quad [cm] \quad and \quad A_{mp-ab} = 2\pi L r_{mp-ab} \quad [cm^2] \qquad (3,4)$$

6

and length of the conduction path, ℓ, by:

$$\ell_{ab} = \frac{r_{cm-b} - r_{cm-a}}{2} \qquad [cm] \tag{5}$$

Finally, intercompartmental conductance, K_{ab}, is calculated from:

$$K_{ab} = \frac{k_a k_b A_{mp-ab}}{(k_a + k_b)\ell_{ab}} \qquad [W \cdot {}^\circ C^{-1}] \tag{6}$$

where k_a and k_b are values of the thermal conductivity for compartments a and b in $W \cdot cm \cdot {}^\circ C^{-1} \cdot cm^{-2}$ (14,30).

Table 1 Assumed distribution of body weight, resting heat production and resting cardiac output for a hypothetical subject ($W = 70$ kg, $A_D = 1.8$ m^2, $\%_{fat} = 14$) and estimated lumped values of specific heat, specific thermal conductivity and conductance for a 6-node cylinderical representation of this subject.

Model Compartment	Distribution of Body Weight, Metabolism and Cardiac Output			Estimated Specific Heat (W·min·g⁻¹·°C⁻¹)	Estimated Thermal Conductivity (W·cm·cm⁻³·°C⁻¹)	Estimated Inter-Compartment Conductance (W·°C⁻¹)
	%W	%M$_{rest}$	%CO$_{rest}$			
Core	32	83	92	51	$5.43 \cdot 10^{-3}$	
						30.3
Muscle	46	12	4	63	$4.18 \cdot 10^{-3}$	
						23.5
Fat	14	4	1	42	$1.59 \cdot 10^{-3}$	
						150.5
Vascular Skin	1	0	3	63	$4.18 \cdot 10^{-3}$	
						20 - 400
Avasculer Skin	5	1	0	63	$2.09 \cdot 10^{-3}$	
Central Blood	2	0	0	62	$4.18 \cdot 10^{-3}$	

A schematic diagram of the passive system with computed dimensions for a hypothetical individual ($W = 70$ kg, $A_D = 1.8$ m^2) is shown in Figure 1 and Table 1 lists values of passive system constants for an individual of this size.

7

Heat Production. Rates of metabolic heat production in the core, fat and avascular skin compartments are assumed to be fixed percentages of total resting metabolism (M_{rot}), as shown in Table 1 (30). Heat production of the muscle layer (H_{mu}) is variable, depending on total energy expenditure (M_{tot}) and external work performed (W). It is assumed that the blood and vascular skin compartments produce no heat at all.

Heat Transfer With Blood. All compartments (except the avascular skin layer) exchange heat with blood flowing through them by convection. Blood enters each tissue compartment at the temperature of the central blood compartment (T_{bl}) and returns to the central blood compartment at the current temperature of the tissue compartment. Thermal mixing in the central blood compartment is instantaneous. There is no heat exchange with blood while in transit to or from the destination compartment and there is no counter-current heat exchange between arterial and venous elements. Rates of blood flow through core (BF_{cr}), through muscle (BF_{mu}) and through vascular skin (BF_{vsk}) are independently controlled by the active system in response to the physiological demands of exercise and thermoregulation. The rate of blood flow through fat (BF_{fat}) is considered to be small (1.2% of basal cardiac output) and unchanging.

Heat Transfer With The Environment. Heat exchange between skin, clothing and environment is assessed using the partitional calorimetric model of Gagge and Nishi (11). Heat is lost from the skin surface by the combined sensible routes of radiation and convection ($R+C$) and by the insensible route of sweat evaporation (E). Heat loss also occurs from the central blood compartment via the respiratory passages through convection and evaporation ($C_{res}+E_{res}$).

Sensible Heat Loss. ($R+C$) is given by:

$$(R+C) = F'_{cl}h(\bar{T}_{sk}-T_o), \qquad [W \cdot m^{-2}] \qquad (7)$$

where h is the combined coefficient for heat transfer by radiation and convection, defined as $h = (h_r + h_c)$. T_o is operative temperature, defined as $T_o = (h_r\bar{T}_r + h_cT_a)/(h)$, and F'_{cl} is a dimensionless climatic efficiency factor, defined as $1/(1 + 0.155I_{clo}h)$. I_{clo} is the clothing insulation value in Burton's clo units, $\bar{T}_r$ is the mean radiant temperature (°C) and T_a is ambient air temperature (°C).

8

h_r is obtained from:

$$h_r = 4\sigma(A/A_D)f_{acl}\left[\frac{(T_{cl}+T_o)}{2} + 273\right]^3, \quad where \quad (8)$$

σ is the Stefan–Boltzman Constant: 5.67×10^{-8} [$W \cdot m^{-2} \cdot K^{-4}$].

(A/A_D) is the fraction of body area exposed to radiation (0.72), and

f_{acl} is the Breckenridge clothing area factor, defined as $(1 + 0.15I_{clo})$ [nd].

T_{cl}, the temperature of the outer clothing surface, is estimated by the expression: $T_{cl} = T_o + F'_{cl}(\bar{T}_{sk} - T_o)$. Formulas used by the program to calculate the convective heat transfer coefficient, h_c, are shown in Table 2. The variables v_{air} and v_{move} are speeds of air around a stationary body and of a body through stationary air, respectively, in m·sec^{-1}.

Table 2. Formulas for calculating h_c, the convective heat exchange coefficient. Adapted from Gagge and Nishi (11).

Activity Level	Formula for h_c
Sitting Rest, Stationary Arm Work	$h_c = 11.6(v_{air})^{0.5}$
Stationary Treadmill Walking	$h_c = 6.5(v_{move})^{0.39} + 1.96(v_{air})^{0.86}$
Free Walking	$h_c = 8.6(v_{move})^{0.53} + 1.96(v_{air})^{0.86}$
Stationary Bicycle at 50 rev·min^{-1}	$h_c = 5.5 + 1.96(v_{air})^{0.86}$

Insensible Heat Loss. E is determined by the rate of sweat secretion ($\dot{m}_{sw}$) and the maximal rate of evaporative heat loss from a fully wetted skin surface (E_{max}). E_{max} is a function of the vapor pressure gradient between the fully wetted skin surface and the air ($P_{s,sk} - P_w$), the evaporative heat transfer coefficient (h_e) and i_m: Woodcock's dimensionless factor for permeability of water vapor through clothing. The evaporative heat transfer

9

coefficient, h_e, is directly related to the convective heat transfer coefficient, h_c, by the Lewis Relation (13).

When evaporation is not restricted by clothing or the environment then $E_{sk} = (\dot{m}_{sw}\lambda)/A_D$ in $W{\cdot}m^{-2}$, where $\dot{m}_{sw}$ is in $g{\cdot}min^{-1}$ and λ is the heat of vaporization for sweat at 35°C: 40.8 $W{\cdot}min{\cdot}g^{-1}$. The expression for E_{sk} under conditions where evaporation of sweat is restricted is (13):

$$E_{sk} = E_{max} = h_e \, F'_{pcl} \, (P_{s,sk} - P_w), \quad \text{for } E_{max} \le \frac{m_{sw}\lambda}{A_C} \qquad [W{\cdot}m^{-2}] \qquad (9)$$

where F'_{pcl} is the modified dimensionless [nd]

Nishi permeation efficiency factor = $\dfrac{h}{h_c} \, F'_{cl} \, i_m$, A_D is the Dubois

surface area and $h_e = 2.2 \, h_c$ (at sea level) $[W{\cdot}m^{-2}{\cdot}Torr^{-1}]$.

$P_{s,sk}$ is related to $\bar{T}_{sk}$ by the Antoine Equation (13):

$$P_{s,sk} = \exp\left(18.6686 - \frac{4030.183}{T_{sk} + 235}\right) \quad [Torr] \qquad (10)$$

Respiratory Heat Loss. $(C_{res}+E_{res})$ is directly related to ventilation rate which, in turn, is directly related to aerobic exercise intensity (M_{tot}) up to maximal levels. The combined equation for convective and evaporative respiratory loss is taken from Fanger (9):

$$(C_{res}+E_{res}) = M_{tot}[0.0014(34 - T_a) + 0.0023(44 - P_w)] \quad [W{\cdot}m^{-2}] \qquad (11)$$

10

Compartmental Heat Balance. The usual conservation of energy statements apply and have been described in detail by others (28, 32). The general differential equation describing the rate of change in heat content of the nth annular compartment at any time t is:

$$\frac{d}{dt}Q_n(t) = H_n(t) + \{K_{n-1,n}[T_{n-1}(t)-T_n(t)]\} - \{K_{n,n+1}[T_n(t)-T_{n+1}(t)]\} -$$

$$\{BF_n(t)\cdot\rho_{bl}\cdot c_{bl}[T_n(t)-T_{bl}(t)]\} \quad [W] \tag{12}$$

The specific equations for each solid compartment are:

$$\frac{d}{dt}Q_{cr} = H_{cr} \cdot [K_{cr,mu}(T_{cr}-T_{mu})] - [BF_{cr}\cdot\rho_{bl}\cdot c_{bl}(T_{cr}-T_{bl})] \tag{12a}$$

$$\frac{d}{dt}Q_{mu} = H_{mu} + [K_{cr,mu}(T_{cr}-T_{mu})] - [K_{mu,fat}(T_{mu}-T_{fat})] - [BF_{mu}\cdot\rho_{bl}\cdot c_{bl}(T_{mu}-T_{bl})] \tag{12b}$$

$$\frac{d}{dt}Q_{fat} = H_{fat} + [K_{mu,fat}(T_{mu}-T_{fat})] - [K_{fat,vsk}(T_{fat}-T_{vsk})] - [BF_{fat}\cdot\rho_{bl}\cdot c_{bl}(T_{fat}-T_{bl})] \tag{12c}$$

$$\frac{d}{dt}Q_{vsk} = H_{vsk} + [K_{fat,vsk}(T_{fat}-T_{vsk})] - [K_{vsk,sk}(T_{vsk}-T_{sk})] - [BF_{vsk}\cdot\rho_{bl}\cdot c_{bl}(T_{vsk}-T_{bl})] \tag{12d}$$

$$\frac{d}{dt}Q_{sk} = H_{sk} + [K_{vsk,sk}(T_{vsk}-T_{sk})] - A_D[(R+C) + E] \tag{12e}$$

and for the central blood compartment:

$$\frac{d}{dt}Q_{bl} = \rho_{bl}c_{bl}\{[(T_{cr}-T_{bl})BF_{cr}] + [(T_{mu}-T_{bl})BF_{mu}] + [(T_{fat}-T_{bl})BF_{fat}] +$$

$$+ [(T_{vsk}-T_{bl})BF_{vsk}]\} - \{C_{res}+E_{res}\} \tag{12f}$$

Each differential equation is evaluated by a simple numerical integration procedure that is based on the assumption that if Δt is made very small, then the value of dQ_n/dt at time t_m is approximately the same as the value of $\Delta Q_n/\Delta t$ over the interval: $(t_m-\Delta t)$ to t_m (10,31).

11

Then the change in heat content of compartment n, ΔQ_n, is obtained using the following approximation:

$$\Delta Q_n(t_m)\big|_{t_m-\Delta t}^{t_m} \approx \frac{d}{dt}Q_n(t_m)\,\Delta t \qquad [W\cdot min] \qquad (13)$$

From this, $\Delta T_n(t_m)$ is calculated from:

$$\Delta T_n(k_m) = \frac{\Delta Q_n(k_m)}{\rho_n c_n V_n} \qquad [C^\circ \text{ or } K]$$

where ρ_n, c_n, and V_n are the density, heat

capacity, and volume of the nth compartment.

(14)

At any chosen time of interest (t_i) the temperature of the n_{th} compartment is obtained by iteration:

$$T_n(t) = T_{n_o} + \sum_{k=1}^{k=i}\Delta T_n(k), \qquad [^\circ C]$$

$$\text{where } i = \frac{t_i}{\Delta t} + 1$$

and T_{n_o} is the initial temperature condition.

(15)

There would rarely be reason to choose successive values of t_i less than 0.25 min apart and Δt is initially set by the program at 0.025 min, thus providing a minimum of 10 iterations per reporting interval. Under most circumstances this iteration rate is adequate to satisfy the assumptions regarding the use of Equation 13. However, if $\Delta T_n > 0.1$ C$^\circ$ during any interval then Δt is automatically reduced by the program for the remainder of interval t_i according to the formula:

$$\Delta t_{new} = \frac{(0.1)(\Delta t_{old})}{|\Delta T_n|} \qquad (16)$$

Δt is automatically reset to 0.025 min for the beginning iteration in the next time of interest period (t_2).

Active System

The active system consists of mathematical algorithms that describe the behavior of physiological effectors whose outputs attempt to control internal temperature by redistributing blood flow and among tissue elements and by increasing the potential for environmental heat loss by increasing sweat secretion. On occasion, increased thermogenesis from shivering may be activated. Inputs to the simulation's active system include temperature levels within the passive system, primarily from the central blood compartment (T_{bl}) and from skin ($\bar{T}_{sk}$) and also inputs from age, energy expenditure (M_{tot} or $\dot{V}O_2$) and from heat production (H_{tot}). Effectors include rates of blood flow and convective heat flow among four of the five tissue compartments, conductance between vascular and avascular skin compartments, the rate of sweating and the rate of shivering. Also the level of cardiac stroke volume, which is influenced by both work intensity and thermal factors, is controlled. Active system algorithms and values of heat exchange between skin, clothing and the environment are recalculated during each iteration.

Change-of-State Lags

Discontinuities in physiological responses occurring during the transition between exercise levels can be particularly troublesome when there are large changes in workload. First-order lags are introduced so as to restrain large, sudden changes in calculated blood flows and stroke volume that would otherwise accompany change-of-state discontinuities. These lags are described by:

$$X_{m+1} = X_m + (X_{ncv} - X_m)\left[1 - \exp\left(\frac{-0.693\,t_m}{t_{0.5}}\right)\right], \quad where \qquad (17)$$

X_{m+1} is the new time-lagged value for variable X, X_m is the time-lagged value for X during the last iteration interval, X_{ncv} is the new non-lagged value for X as calculated by the algorithm, t_m is the elapsed time into the current time of interest period and $t_{0.5}$ is the response half-time (from 30 sec to 2 min, depending upon the function).

13

Skin Blood Flow

The rate of thermoregulatory skin blood flow (BF_{vsk}) is described primarily as a linear function of change in hypothalamic temperature from a reference point, but is also modulated by skin temperature ($\bar{T}_{sk}$), by posture, by exercise intensity and, transiently, to the initiation and cessation of exercise (4, 17-19, 23). The algorithm used in the present simulation for control of BF_{vsk} is based primarily on an empirical regression model suggested by Roberts and Wenger during upright exercise and heat stress, but also incorporates effects of activity level as inferred from other work (18, 23).
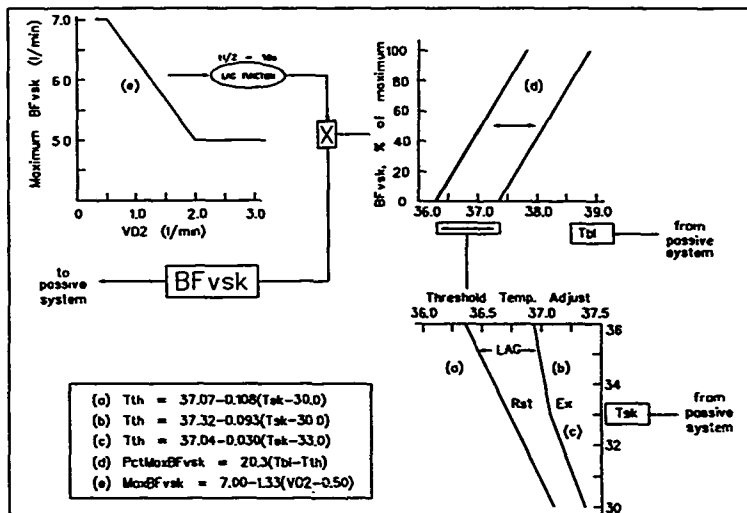

Figure 1. Algorithm for calculating BF_{vsk}. Maximum is determined by activity (e), threshold by activity & $\bar{T}_{sk}$ and level by T_{bl}. Lags introduced by Eq. 17.

A quantitative representation of this control algorithm is diagrammed in Figure 2. BF_{vsk} is modeled as a linear function of central blood temperature (T_{bl}). Both $\bar{T}_{sk}$ and exercise shift this function's intercept on the T_{bl} axis: increasing $\bar{T}_{sk}$ reduces the value of T_{bl} necessary to produce a given value of BF_{vsk} while exercise increases the value of T_{bl} required to produce a given value of BF_{vsk}. Exercise also produces graded reductions in maximal skin blood flow: from 7.0 l•min⁻¹ at rest to 5.0 l•min⁻¹ at a $\dot{V}o_2$ of 2.0 l•min⁻¹ (18). Minimum BF_{vsk} during intense vasoconstriction is set at 30 ml•min⁻¹. The assumption is

14

made that all "rest" is in the upright seated position and that all "work" is in the upright standing position.

Vascular-Avascular Skin Conductance

Cutaneous veins are quite distensible and fill with blood as BF_{vsk} increases (26). An increase in transit time of blood through the cutaneous venous bed would presumably accompany this venous distension, resulting in greater heat transfer between blood and skin. Effectively, then, the value for conductance between these layers ($K_{vsk,sk}$) increases as BF_{vsk} increases. To date, there is no direct evidence to document the nature of the relationship between BF_{vsk} and $K_{vsk,sk}$. The presumption is made here that each ten-fold increase in BF_{vsk} increases $K_{vsk,sk}$ by a fixed amount (19). The maximal value for $K_{vsk,sk}$ was obtained rationally by calculation, assuming maximal vasodilation and perfect thermal contact (Equation 6 and Table 1). The minimum value, 10 $cm^3 \cdot m^{-2} \cdot min^{-1}$, assumes maximal vasoconstriction, so that for heat transfer purposes the vascular skin layer is essentially bloodless and similar to the avascular skin layer. $K_{vsk,sk}$, modeled as a function of log BF_{vsk}, is shown in Figure 3.
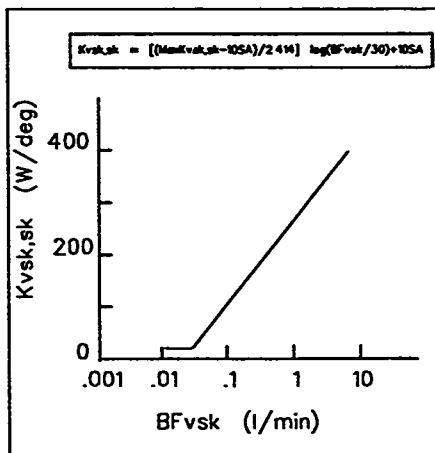

Figure 3. Hypothetical relationship between skin blood flow and skin conductance.

Core Blood Flow

While the core contains the skeletal system, the nervous system and connective tissue, these components make negligible demands on cardiac output. The core

15

components receiving the largest blood flows at rest are kidneys and splanchnic regions which obtain over a third of the resting cardiac output. With the addition of exercise and/or heat stress, blood flow to splanchnic and renal vasculatures can be reduced by as much as 70% (26).
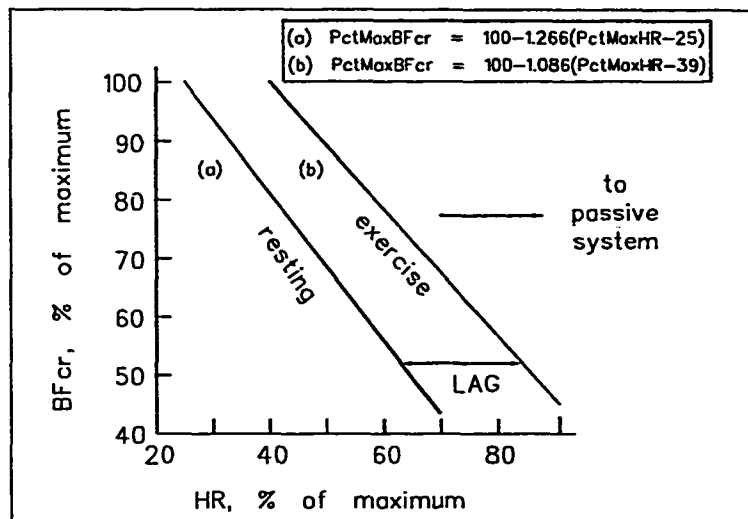

$$(a) \quad PctMaxBFcr = 100 - 1.266(PctMaxHR - 25)$$
$$(b) \quad PctMaxBFcr = 100 - 1.086(PctMaxHR - 39)$$

Figure 4. BF_{cr} is calculated from an observed empirical association with heart rate. Basal BF_{cr} assumed to be 92% of basal cardiac output. From Rowell (25).

The paradigm for controlling core or visceral blood flow (BF_{cr}) is based on a regression model of splanchnic and renal blood flow on heart rate (Figure 4) that stems from many observations taken during rest and exercise with and without heat stress (25). The data fall on two nearly parallel lines (one for rest and another for exercise) regardless of whether heart rate was elevated by heating or by lower body negative pressure. Although it is unlikely that decrements in BF_{cr} are linked causally to increments in HR, the operational assumption is made that they are both well-related to a third variable that is independent of blood flow.

16

Muscle Blood Flow

This model for the control of BF_{mu} is a function of (a) the oxygen requirements of skeletal muscle ($Mu\dot{V}O_2$), (b) the demands for total cardiac output (CO_{req}), (c) the maximal cardiac output (CO_{max}) and (d) the level of oxygen extraction from the blood ($PctO_2ext$). In general, BF_{mu} is assumed to be a linear function of $Mu\dot{V}O_2$; $PctO_2ext$ is assumed to be 60 percent and CO_{req} is assumed to be less than CO_{max} (Figure 5). If CO_{req} at anytime becomes greater than CO_{max}, then $PctO_2ext$ is incrementally increased to force compensatory reductions in BF_{mu}. The change in $PctO_2ext$ is based, in part, on a hypothetical scheme proposed by Rowell (26). As shown in Figure 5, $Mu\dot{V}O_2$ can be impacted by both activity level and shivering thermogenesis.
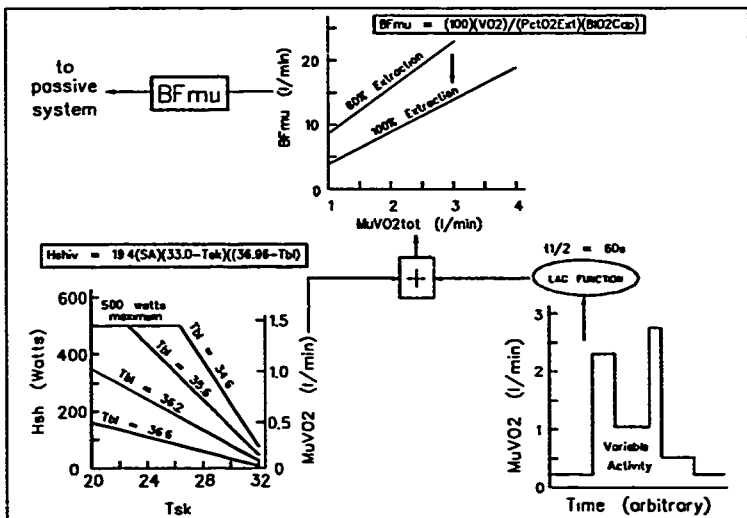

Figure 5. BF_{mu} is a function of muscle O_2 consumption. Percent extraction variable depending on competing demands for cardiac output. Shivering model from (31).

17

Cardiac Stroke Volume

Stroke volume (SV) is a complicated function whose value is influenced by many factors. Only two are considered here: the level of exertion and the level of skin temperature, as shown in Figure 6. Starting at rest, assumption of upright posture displaces central intravascular volume to the periphery, thus reducing filling pressure and SV. At this point maximal stroke volume (SV_{max}) is at its lowest, about 85 cm^3 (26). Beyond this, (SV_{max}) increases directly with activity level, up to a $\dot{V}O_2$ of about 2 $\ell\cdot$min^{-1} where it attains a high of about 130 cm^3 (2).

When $\bar{T}_{sk}$ is high, SV can be diminished because of displacement of central
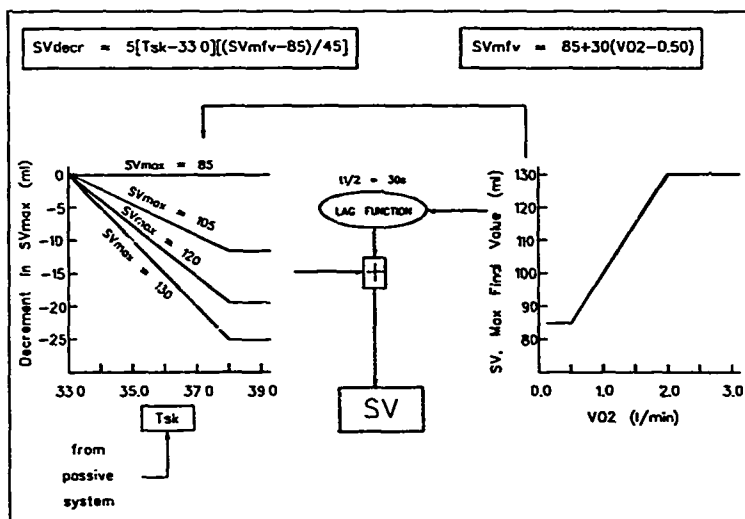

Figure 6. Upright cardiac stroke volume is modeled as a function of the level of exertion and of skin temperature. Lag function described by Eq. 17.

intravascular volume into cutaneous veins (25). This aspect of SV control is modeled in the following way. At rest this displacement effect is nil; the value of SV is equal to resting SV_{max} regardless of the magnitude of $\bar{T}_{sk}$. As energy expenditure and SV_{max} increase, the impact of increasing $\bar{T}_{sk}$ becomes more pronounced and the final value of SV can be as

much as 25 ml lower than when $\bar{T}_{sk}$ is cool. It is cautioned that the quantitative aspects of this strategy are largely hypothetical.

Cardiac Output and Heart Rate

At any instant the actual cardiac output (CO) is the smaller of required cardiac output (CO_{req}) and maximal cardiac output (CO_{max}). Heart rate (HR) is a variable determined simply by the ratio of present values for CO and SV. CO_{req} is determined by the sum of required blood flows to all compartments. CO_{max} is determined by the product of maximal heart rate (HR_{max}) and the current value for SV (Figure 7). HR_{max} is computed from the approximate guideline: $HR_{max} = 220 - age$ (1).
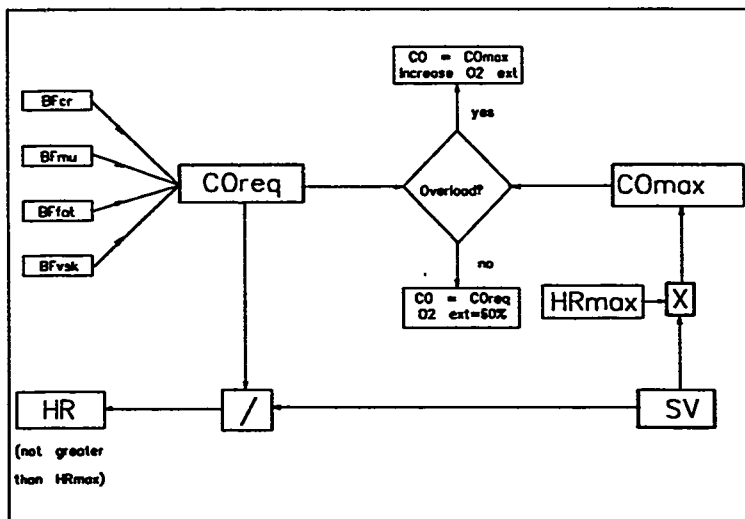

Figure 7. Relationship between CO_{req} and CO_{max}. Rate of muscle O_2 extraction can be increased by excessive demand for cardiac output.

Sweating Rate and Shivering

The sweating rate algorithm is that proposed by Nadel *et al.* (22) as a function of hypothalamic temperature (T_{bl}) and $\bar{T}_{sk}$:

$$\dot{m}_{sw} = A_D\left(4.83[T_{bl}-T_{bl_*}] + 0.56[\bar{T}_{sk}-\bar{T}_{sk_*}]\right) \exp\left(\frac{\bar{T}_{sk}-\bar{T}_{sk_*}}{10}\right) \quad (18)$$

Threshold temperatures T_{bl} and for $\bar{T}_{sk}$ are set at 36.96°C and 33.00°C, respectively.
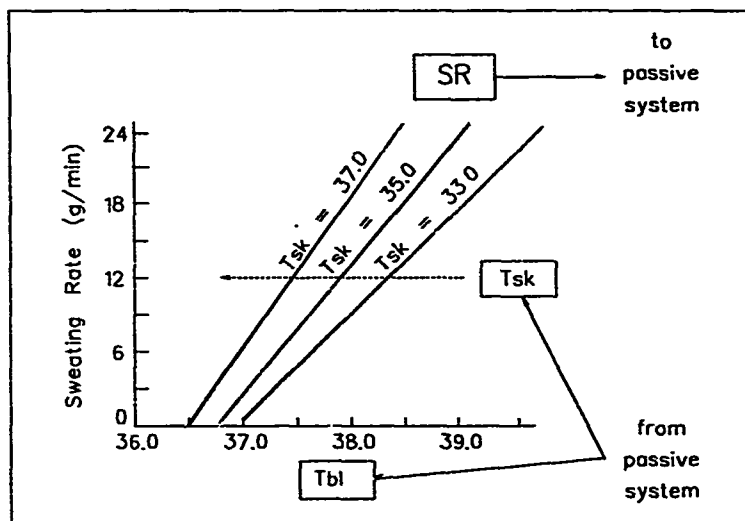
Figure 8. Diagrammatic representation of the sweating rate algorithm (Eq. 18). From Nadel et al. (22).

Although this simulation is not designed for use during obvious cold exposure, shivering can occur under room temperature conditions when persons are recovering from heavy exercise or heat exposure. Therefore a shivering algorithm. originally proposed by Stolwijk and Hardy and shown in Figure 5, was included in the simulation (31).

Model Implementation

A flow chart summarizing the basic elements of program flow is shown in Figure 9. The simulation was developed as an interactive program and compiled in a structured BASIC dialect (Turbo BASIC 1.1, Borland International, Inc., Scotts Valley, CA) but any common programming language should be satisfactory. Program inputs include subject anthropometric data (stature, weight, age, percent body fat), clothing insulation and water vapor permeability, environmental variables (air temperature, humidity and movement), type and intensity of exercise (leg work, arm work or rest; walking speed and grade or energy expenditure), and length of time cycles.

Validation of the Simulation

Data from seven studies emphasizing various aspects of exercise under heat stress were chosen to test the simulator. Selected studies, representing different investigators and laboratories, presented enough detail about subjects, measurement methods, activity levels, and environmental conditions so that the protocol could be accurately input to the simulator. Six of the studies included tabular data and the standard deviation statistic or included individual subject data so that this statistic could be calculated. Data from none of these studies had been used in development of the simulator.

Data Set 1.: Ekblom *et al.* (7). Three well-trained subjects clothed in shorts exercised by continuously cycling at 60% $\dot{V}O_2$max in a comfortable (21°C) environment. Air movement was rapid to insure free evaporation. Data for T_{re}, $\bar{T}_{sk}$ and HR were available at 50 min of exercise and HR and were compared to simulator outputs programmed for that time. This data set tests the simulator response to exertion without external heat stress.

Data Set 2.: Gonzalez *et al.* (12). Five subjects clothed in shorts each exercised in 16 experiments on a bicycle ergometer at 28% $\dot{V}O_2$max. In each experiment subjects were exposed to a different combination of temperature and humidity chosen to produce one of six effective temperature (*ET*) states. Tabulated steady-state values for T_{es}, $\bar{T}_{sk}$ and HR
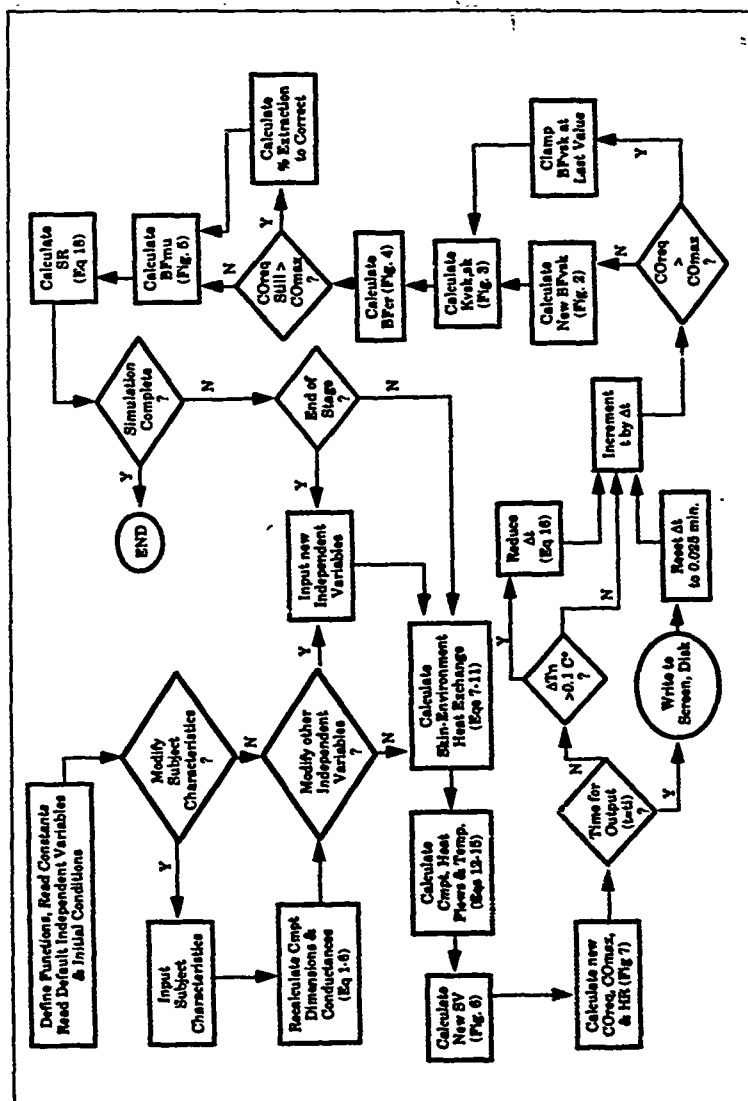
21

Figure 9. Flow chart of main program elements in the simulation. Calculated values are reported at multiples of t_v

22

at 40 min were compared with simulator outputs at the same time. This data set tests the simulation with respect to a wide range of environments without the complicating effects of changing workload.

Data Set 3.: Kraning and Gonzalez (20). Four subjects exercised in a warm environment (30°C, 25% RH) for 60 min under four protocols: continuous treadmill walking (1.34 m·s⁻¹, 3% grade) while wearing shorts or heavy semi-permeable clothing and repeated cycles of walking (1.34 m·s⁻¹, 0% grade for 4 min), jogging (2.24 m·s⁻¹, 5% grade for 2 min) and rest (seated for 4 min) while again wearing either shorts or heavy semi-permeable clothing. This data set provided measurements to illustrate the time course of responses to mild, fully compensable external heat stress and to severe, uncompensable external heat stress during two different patterns of internal heat production. Data were reported at 15 second intervals for T_{re}, $\bar{T}_{sk}$ and for HR and averaged across subjects. Each averaged 15 second data point was compared with its corresponding simulator output over a 60 min period.

Data Set 4.: Pandolf *et al.* (unpublished observations). 10 subjects wearing shorts rested for 10 min in a hot, dry (49°C, 20% RH) environment then worked in the same environment on a stationary ergometer at a workload requiring 53% $\dot{V}O_2$max for 50 min more. This data set illustrates the physiological consequences of heavy work under desert-like conditions and is typical of responses observed on the first day of heat acclimation. As in Data Set 3., T_{re} and $\bar{T}_{sk}$ were compared with simulator outputs every 15 seconds for 60 min. HR data were available for comparison at 10 min intervals.

Data Set 5.: Rowell *et al.* (24). Average central circulatory and thermal responses of 6 subjects exercising at 31% $\dot{V}O_2$max and 5 subjects exercising at 54% $\dot{V}O_2$max were measured while $\bar{T}_{sk}$ was driven between 28°C and 40°C with a temperature controlled, water perfused suit. In simulating this data set $\bar{T}_{sk}$ was made a forcing function rather than a dependent variable, and equations describing heat exchange with the environment and clothing were eliminated. $\bar{T}_{sk}$ was independently calculated during each iteration interval using a set of best-fit polynomial regression equations that duplicated the skin temperature response of the original data set. Using this data set it was possible to compare directly data and simulation outputs for T_{bl}, and for HR, SV and CO at 5 min intervals.

23

Data Set 6.: Saltin et al. (27). Four trained subjects exercised in separate experiments at either 27%, 46% or 72% $\dot{V}O_2$max in an ambient temperature of either 10°C, 20°C, or 30°C. Reported data for T_{re}, $\bar{T}_{sk}$ and for HR at the end of each exposure (50 min) were compared with simulator outputs.

Data Set 7.: Skölderström (29). Eight fire fighters each exercised by walking for one hour at 2 workloads (21% and 31% $\dot{V}O_2$max) in 4 experiments while wearing either coveralls or fire fighting turnout gear in a 15°C or a 45°C environment. Reported end values for T_{re}, $\bar{T}_{sk}$ and for HR at 60 min were compared with simulator outputs.

Statistical Method

A summary statistic, the root mean squared deviation (rmsd), was proposed by Haslam and Parsons to compare values of simulated variables with average values of experimental variables at corresponding time points (15). The rmsd statistic is defined as:

$$rmsd = \sqrt{\frac{1}{n} \sum_{i=1}^{n} d_i^2} \quad where:$$

d_i = difference between observed and predicted at each time point
n = number of comparison time points.

This statistic is comparable with the average standard deviation (sd) of the data set. The ave sd was available for all but Study No. 5.

Results

Comparisons of values for the sd of experimental data and the rmsd between experimental data averages and simulator outcomes are detailed in Table 3 and summarized in Figure 10. For three of the studies (No. 1, No. 6 and No. 7) each reported value for the sd and the rmsd represents a single end-point comparison at each condition. In one study (No. 2) each value of the sd and the rmsd reported represents the average of 2 to 3 end-points at each condition. In two studies (No. 3 and No. 4) each reported value of the sd and of the rmsd represents the average of comparisons at 15 second intervals for the entire time course: 240 and 200 comparisons, respectively. In one study (No. 5) the reported average rmsd is based on 21 comparisons during the time course of the experiment and values for the sd were not available.
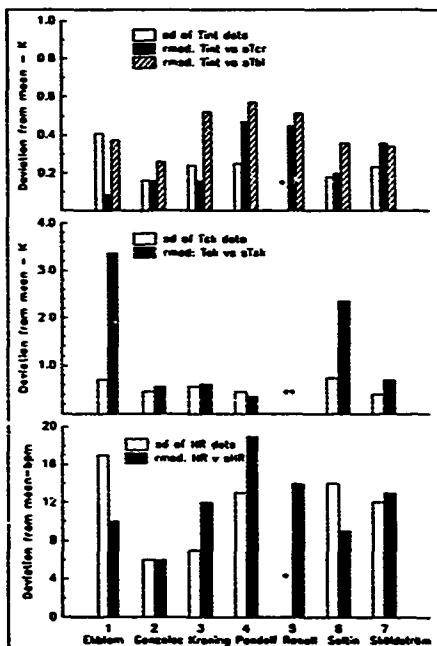

Figure 10. Comparison of data standard deviations with rms deviations. `sd not available. ˜T_{sk} controlled.

TABLE 3. Simulator performance characteristics. Simulator outputs for internal and skin temperatures and for heart rate are compared with corresponding means and standard deviations of data from seven independent studies.

Study	n,m	Internal Temperature (°C)			Skin Temp.(°C)		Heart Rate (bpm)	
		ave sd Tint	rmsd Tint vs sTcr	rmsd Tint vs sTbl	ave sd Tsk	rmsd Tsk vs sTsk	ave sd HR	rmsd HR vs aHR
1. Ekblom et al. (7)		(Tre)						
480 W·m², 7.5 Torr, 21° C	3,1	0.41	0.00	0.37	0.70	3.37	17	10
2. Gonzalez et al. (12)		(Tes)						
ET = 27.8°C	5,2	0.13	0.23	0.10	0.70	1.65	7	6
32.8°C	5,3	0.12	0.24	0.35	0.57	0.76	5	4
36.8°C	5,3	0.08	0.13	0.42	0.37	0.22	5	3
40.5°C	5,3	0.15	0.06	0.38	0.37	0.29	6	5
43.5°C	5,3	0.22	0.16	0.15	0.30	0.34	8	9
44.0°C	5,1	0.24	0.14	0.17	0.40	0.17	8	6
(All at 210 W·m²)	mean	0.16	0.16	0.26	0.45	0.57	6	6
3. Kraning & Gonzalez (20)		(Tre)						
Continuous work: 172 W·m², free evap.	4,240	0.17	0.18	0.47	0.79	0.39	3	7
Continuous work: 172 W·m², limited evap	4,240	0.23	0.28	0.39	0.37	0.85	8	9
Work/Rest: 52/156/417 W·m², free evap	4,240	0.26	0.06	0.50	0.68	0.66	7	12
Work/Rest: 52/156/417 W·m², limited evap	4,240	0.29	0.11	0.70	0.41	0.56	10	18
(All at 8 Torr, 30°C)	mean	0.24	0.16	0.52	0.56	0.62	7	12
4. Pandolf et al. (unpublished)		(Tes)						
360 W·m², 18 Torr, 49°C	10,200	0.25	0.47	0.57	0.46	0.37	13	19
5. Rowell et al. (24)		(Tbl)						
200 W·m², Tsk 28°C - 41°C	6,21	no sd	0.51	0.58	no sd	—	no sd	12
400 W·m², Tsk 28°C - 41°C	5,21	no sd	0.39	0.44	no sd	—	no sd	15
(Tsk controlled by water-perfused suit)	mean	—	0.45	0.51	—	—	—	14
6. Sakin et al. (27)		(Tre)						
193 W·m², 10°C	4,1	0.17	0.18	0.15	0.83	0.54	9	12
20°C	4,1	0.13	0.22	0.13	0.27	1.04	9	10
30°C	4,1	0.22	0.17	0.18	0.62	1.30	6	13
333 W·m², 10°C	4,1	0.24	0.10	0.59	0.32	2.60	7	4
20°C	4,1	0.18	0.00	0.41	0.45	3.46	9	4
30°C	4,1	0.20	0.13	0.31	0.91	0.96	16	2
520 W·m², 10°C	4,1	0.17	0.12	0.74	1.49	4.83	24	15
20°C	4,1	0.13	0.16	0.52	1.16	3.52	20	14
30°C	4,1	0.17	0.76	0.29	0.65	2.26	23	11
(All < 13 Torr)	mean	0.18	0.20	0.36	0.74	2.37†	14	9
7. Skoldstrom (29)		(Tre)						
137 W·m², 2 Torr, 15°C, coveralls	8,1	0.20	0.23	0.06	0.3	0.3	7	17
205 W·m², 2 Torr, 15°C, fire gear	8,1	0.20	0.14	0.20	0.4	0.6	12	12
137 W·m², 11 Torr, 45°C, coveralls	8,1	0.20	0.07	0.26	0.4	1.3	10	10
205 W·m², 11 Torr, 45°C, fire gear	8,1	0.30	1.01	0.82	0.4	0.5	18	12
mean		0.23	0.36	0.34	0.4	0.7	12	13
AVERAGE OVER STUDIES		0.25	0.28	0.42	0.55	1.33	12	12

Temperatures: Tre = rectal, Tes = esophageal, Tbl = central blood, Tcr = core, Tsk = skin. The prefix s indicates simulator output, sd = standard deviation and rmsd = root mean square deviation between data mean and simulated variable. n = number of subjects and m = number of paired data-simulation values used to calculate rmsd. † sTsk was consistently greater than Tsk.

Internal Temperature

In 1 study (No. 5) internal temperature (T_{int}) was taken as blood temperature in the right atrium (T_{ra}), in 2 studies (No. 2 and No. 4) as esophageal temperature (T_{es}) and in the remaining 4 studies as rectal temperature (T_{re}). The overall average sd for internal temperature was 0.25°C. The rmsd statistic for T_{int} vs. T_{cr} was generally smaller than the rmsd statistic for T_{int} vs. T_{bl} (Figure 10). The average rmsd for T_{int} vs. T_{cr} was 0.28°C and the average rmsd for T_{int} vs. T_{bl} was 0.42°C.

Mean Skin Temperature

Study No. 5 was not included because $\bar{T}_{sk}$ was controlled as an independent variable. The average sd for $\bar{T}_{sk}$ was 0.55°C while the average rmsd statistic was 1.33°C. In 4 of the 6 studies the sd and rmsd were in close agreement but in 2 studies (No. 1 and No. 6) there was substantial disagreement; the simulation consistently overpredicted $\bar{T}_{sk}$ (Figure 10). The subjects of these two studies were reported to be in a high state of physical training. Since physical training confers a degree of heat acclimation, perhaps these individuals had an earlier onset of sweating and a lower $\bar{T}_{sk}$ than would be expected for non-acclimated subjects.

Heart Rate

The value of the average rmsd statistic for mean heart rate vs simulator output was the same as the value of the average sd (12 beats•min^{-1}) although both the sd and the rmsd were quite variable between studies.

Sample Plots of Simulator Outputs

The sd and rmsd error statistics are standard metrics for comparing the overall precision of the simulator with the observed variance of experimental data; however, taken alone such comparisons fail to identify problems of tracking or consistent underprediction or overprediction. Correct tracking is particularly important when protocols include changes in energy expenditure or environmental conditions. Figure 11 shows the time course of ten selected simulator outputs and three experimental counterparts for Study 4. Panel *a* shows predicted heat production at rest and while cycling. Panel *b* compares the time course of T_{es} ± sd with simulator outputs for T_{cr} and T_{bl}. Both simulator temper-
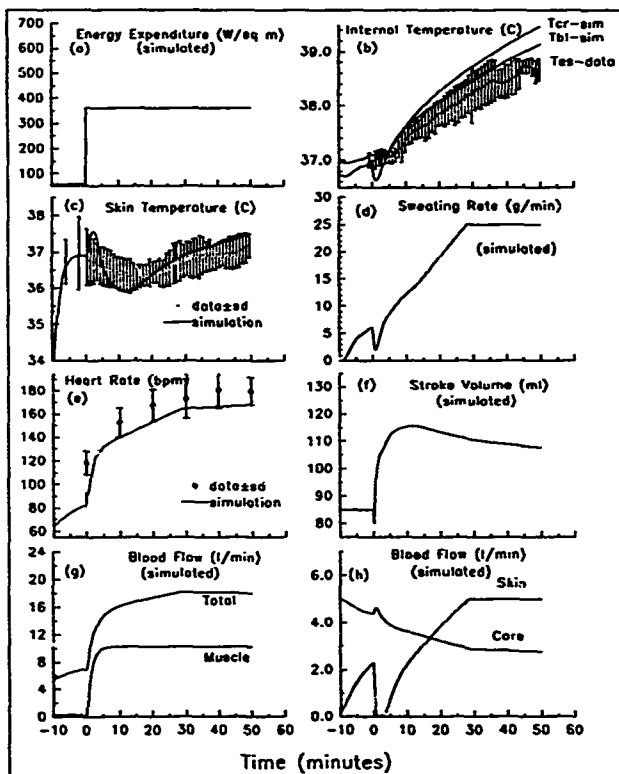

Figure 11. Time course of selected simulator outputs and 3 experimental counterparts for Study No 4.

28

atures overpredicted the value T_{es} but T_{bl} was better both in quantitative agreement and in tracking. Panel *c* compares the simulation output and data for average $\bar{T}_s \pm$ sd. Although the simulation tracked the features of the data average, its course was quite exaggerated. Quantitatively, however, the rmsd was slightly smaller than the data sd. Panel *e* shows average HR data $\pm$ sd collected at 10 min intervals compared with 15 second output from the simulator. Although the simulation consistently underpredicted HR, time-course tracking was reasonable.

Figure 12 shows the time course of the same variables for the fourth protocol of Study 3: a highly stressful intermittent work routine. Panel *a* shows the time course of predicted heat production corresponding to cycles of walking, jogging and recovery. Panel *b* compares the time course of average $T_{re} \pm$ sd with simulator outputs for T_{cr} and T_{bl}. Although T_{cr} slightly underestimated T_{re}, tracking was good and small oscillations
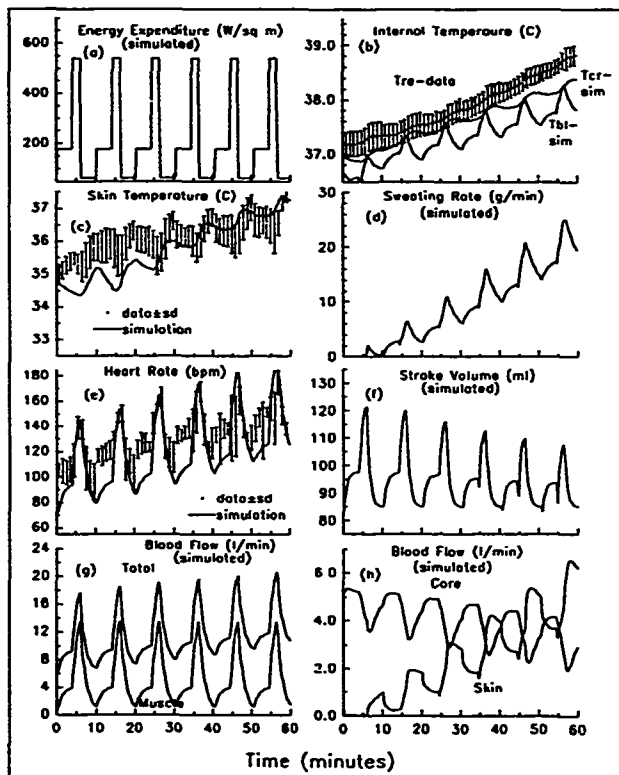

Figure 12. Selected simulator outputs and 3 experimental counterparts from one segment of Study No. 3.

29

of the two temperatures with workload were in phase with each other and similar in magnitude. The average rmsd was 0.11°C compared to an average data sd of 0.29°C. On the other hand, there was poor correspondence between T_{bl} and T_{re}. The average rmsd was 0.70°C and T_{bl} was consistently lower in value than either T_{re} or T_{cr}. Qualitatively, T_{bl} was quite different than T_{re}, showing a three component waveform with crests and troughs that were more peaked, larger in magnitude, and out of phase with T_{re}. This discrepancy was not entirely unexpected since heat exchange between the muscle and the central blood compartments is affected directly and immediately by large swings in muscle blood flow accompanying changing exertion level (panel g).

Panel c compares the time course of average $\bar{T}_{sk} \pm$ sd with the corresponding simulator output. Average rmsd (0.56°C) was slightly greater than average data sd (0.41°C). Qualitatively, pulsations in data and simulator output accompanying changes in workload were similar in phase, waveshape and magnitude.

Panel e compares the time course of average HR $\pm$ sd and the simulator output for HR. Waveshape and phase relations were similar for data and simulation. On the whole, an ave sd of 10 bpm compared with an rmsd of 18 bpm. Reasonable magnitude agreement was achieved during heavy exercise and recovery phases. However, during the moderate exercise periods the simulator always · derpredicted the level of average HR. Since, in this simulation, HR is not controlled but is simply the quotient of CO and SV, the error must lie either in underestimating the level of CO or in overestimating the level of SV or in both. Since neither CO or SV were measured in this study, the source of error cannot be determined.

Figure 13 is a plot using data from the second protocol of Study 5 where subjects exercised continuously and $\bar{T}_{sk}$ was independently controlled with a water-perfused suit. In the simulation, control of $\bar{T}_{sk}$ was achieved by dividing the skin temperature data curve into 4 time segments, finding the best-fit 5th order polynomial expressions for each segment and then substituting these 4 equations for the previous definition of $\bar{T}_{sk}$ (Equation 15). This procedure gave good agreement between the experimental and simulated $\bar{T}_{sk}$ forcing functions (Panel c). Panel a shows that simulator heat production was constant except for a small increase from shivering (< 1%) when $\bar{T}_{sk}$ fell below 32°C. Panel b shows the time course for average T_{bl}, measured in the right atrium, for T_{re}, and

for simulator generated T_{bl} and T_{cr}. Both simulator outputs tracked average T_{bl} reasonably well but both outputs overshot peak average T_{bl} observed during skin heating by a large amount. 0.5°C. Overall, tracking between average T_{bl} and simulated T_{bl} was somewhat better than between average T_{bl} and simulated T_{cr}. T_{re} was more sluggish than average T_{bl} or either of the simulated temperatures, particularly during rapid skin cooling.

Tracking between simulated and average CO (panel *g*) was also reasonable, especially during skin heating, although simulated CO reached an equilibrium level earlier. However, during rapid skin cooling, average CO declined more slowly than simulated CO. At the same time. simulated SV rose much faster and to a greater extent than average SV (panel *f*). The combined effect of underpredicting CO and overpredicting SV during rapid skin cooling was that simulated HR (Panel *e*) declined far more than the observed
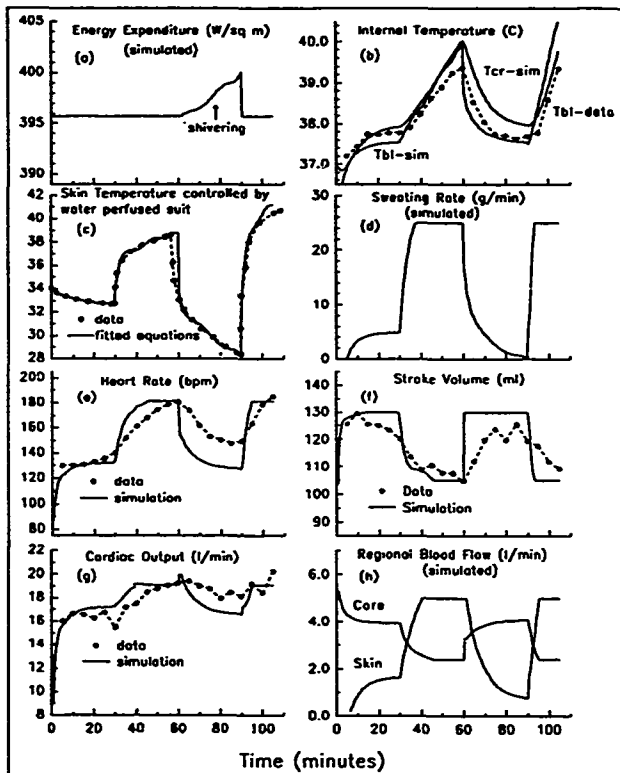

Figure 13. Time course of selected simulator outputs and 6 experimental counterparts from the second part of Study No. 5.

average HR. Tracking of both SV and HR was better during rapid skin heating than during

31

rapid skin cooling.

Discussion

This paper documents the development schemes of a relatively simple computer simulation of thermoregulation designed to predict the time-course of certain critical body temperatures and physiological variables in response to the demands of exercise and heat stress. The capability of this simulation was measured by comparing outputs with data from seven independent studies. Overall, the variance among subjects and the variance between data and simulation were quite similar, suggesting that, under the conditions tested, the computer simulation may be able to forecast an outcome with the same order of precision as a laboratory study of the same problem.

Every component algorithm in the simulation is an approximation and contains error. For instance, the level of SV is dependent upon many factors but only $\dot{V}O_2$ and $\bar{T}_{sk}$ were included in the present algorithm; values for BF_{vsk} over the entire body were inferred from measurements at one forearm site; values for $K_{vsk,sk}$ are entirely hypothetical; et cetera. It is somewhat surprising, therefore, that such good agreement was obtained between simulation and experimental data. Part of the reason may lie in the fact that errors in opposite directions may tend to cancel within closed-loop systems. In any case, satisfactory overall agreement should not be construed as a recommendation for the correctness of any particular algorithm.

Several differences between data and simulation that appear to result from systematic errors in estimation of regional blood flow distribution and of SV during transitions in workload and $\bar{T}_{sk}$ were pointed out. It should be emphasized that the algorithms for regional blood flow and SV were developed from a very small database. These problems indicate areas where further research would be worthwhile.

There is one final caveat. This simulation and its component algorithms are descriptive models rather than explanatory models (16). That is, they are "empirical black boxes" that are used to describe functional relationships between certain thermal and physiological

32

responses and there is no attempt here to imply direct causal relationships between inputs and outputs.

SUMMARY AND CONCLUSIONS

1. This report documents a new computer simulation of physiological and biophysical function designed to aid in forecasting the time course of responses to various combinations of climate, clothing and exercise intensity. The body is modeled as a single cylinder containing five concentric annular tissue compartments (core, muscle, fat, vascular skin and avascular skin) and an interconnecting central blood compartment. Algorithms, dependent upon body temperatures and exercise level, control compartmental blood flows, stroke volume, sweating rate and shivering. Surface heat exchange between clothing and environment is calculated using the accepted techniques of partitional calorimetry. Inputs include environmental variables, clothing parameters, workload and anthropometric data. Outputs include compartment temperatures and blood flows, heart rate, stroke volume, sweating rate, fluid loss and heat storage.

2. Comparison of simulator outputs for core and skin temperatures and heart rate with average data from seven independent studies indicates reasonable agreement; on the whole, differences between data means and simulation outputs were no greater than the data standard deviations.

3. Validation of the simulation in general does not automatically verify the physiological control algorithms incorporated within the simulation, since in complex systems errors in system elements may be in opposite directions and cancel. Systematic discrepancies in heart rate prediction and data in two of the validation studies suggest systematic errors in either underpredicting cardiac output or overpredicting stroke volume during recovery from the stress of heavy exercise or of high skin temperature. In either case, it should be reemphasized that only a scanty database based on a handful of studies was available to develop the algorithms that control regional blood flow and stroke volume.

33

RECOMMENDATIONS

1. Studies are recommended to determine the relationship between stroke volume magnitude with changes in posture, workload and recovery, under conditions of cool and elevated skin temperature.

2. At present, the simulation does not take into account relationships between progressive dehydration, reduction in plasma volume and decrements into stroke volume. Under certain conditions the state of hydration may be an important factor in determining tolerance time, the level of cardiovascular function and the level of core temperature. Efforts to incorporate the effects of hydration status into the simulation should be encouraged.

3. The present model does not attempt to generate a single index datum representative of heat stress, heat strain, tolerance or survival time but the pattern of physiological responses accompanying exposure. It is up to qualified professional personnel to interpret simulator outcomes. The simulation has been verified by comparison with seven human studies. A larger validation database is needed. Further, the present simulation should be compared with other approaches used to assess the impact of work, clothing and heat stress.

REFERENCES

1. Anonymous. *Exercise Testing and Training of Apparently Healthy Individuals: A Handbook for Physicians.* New York, NY: The Committee on Exercise, American Heart Association, 1972.

2. Åstrand, P.-O., T. E. Cuddy, B. Saltin and J. Stenberg. Cardiac output during submaximal and maximal work. *J. Appl. Physiol. 19*: 268-274, 1964.

3. Bevegard, B. S. and J. T. Shepherd. Regulation of the circulation during exercise in man. *Physiol. Rev. 47*: 178-213, 1967.

4. Brengelmann, G. L. Circulatory adjustments to exercise and heat stress. *Ann. Rev. Physiol. 45*: 191-212, 1983.

5. Brozek, J., F. Grande, J. Anderson and A. Keys. Densitometric analysis of body composition: revision of some quantitative assumptions. *Ann. N.Y. Acad. Sci. 110*: 113-140, 1963.

6. DuBois, E. F. *Basal Metabolism in Health and Disease.* Philadelphia, PA: Lea & Febiger, 1927, p. 133.

7. Ekblom B., C. J. Greenleaf, J. E. Greenleaf and L. Hermansen Temperature regulation during continuous and intermittent exercise in man. *Acta Physiol. Scand. 81*: 1-10, 1971 .

8. Emery, A. F., R. E. Short, A. W. Guy, K. K. Kraning and J. C. Lin. The numerical thermal simulation of the human body when undergoing exercise or non-ionizing electromagnetic radiation. *J. Heat Transfer, Trans. Am. Soc. Mech. Engr. (c) 98*: 284-291, 1976.

9. Fanger, P. O. *Thermal Comfort*, 2nd ed. New York, NY: McGraw-Hill, 1972.

10. Gagge, A. P., J. A. J. Stolwijk and Y. Nishi. An effective temperature scale based on a simple model of human physiological regulatory response. *ASHRAE Trans. 77 (Part 1)*: 247-262, 1971.

11. Gagge, A. P. and Y. Nishi. Heat exchange between human skin surface and thermal environment. In: *Handbook of Physiology, Reactions to Environmental Agents.* Bethesda, MD: Am. Physiol. Soc., 1977, sect. 9, chapt. 5, p. 69-92.

12. Gonzalez, R. R., L. G. Berglund and A. P. Gagge. Indices of thermoregulatory strain for moderate exercise in the heat. *J. Appl. Physiol.: Respirat. Environ. Exercise Physiol. 44*: 889-899, 1978.

13. Gonzalez, R. R. Biophysics of heat transfer and clothing considerations. In: *Human Performance Physiology and Environmental Medicine at Terrestrial Extremes.* Indianapolis, IN: Benchmark Press, 1988, chapt. 2, p. 45-96.

14. Gordon, R. G., R. B. Roemer and S. M. Horvath. A mathematical model of the human temperatures regulatory system - transient cold exposure response. *IEEE Trans. Biomed. Engr. BME-25*: 434 - 444, 1976.

15. Haslam, R. A. and K. C. Parsons. An evaluation of computer-based models that predict human responses to the thermal environment. *ASHRAE Trans. 94, pt.1*: ,1988.

16. Houdas, Y. (1981) Modelling of heat transfer in man. In: *Bioengineering, Thermal Physiology and Comfort.*, New York, NY, Elsevier. p. 111-120.

17. Johnson, J. M. and M. K. Park. Effect of heat stress on cutaneous vascular responses to the initiation of exercise. *J. Appl. Physiol.: Respirat. Environ. Exercise Physiol. 53*: 744-749, 1982.

18. Johnson, J. M. Nonthermoregulatory control of human skin blood flow. *J. Appl. Physiol. 61*: 1613-1622, 1986.

19. Johnson, J. M., G. L. Brengelmann, J. R. S. Hales, P. M. Vanhoutte and C. B. Wenger. Regulation of the cutaneous circulation. *Federation Proc. 45*: 2841-2850, 1986.

20. Kraning, K . K. and R. R. Gonzalez. Physiological consequences of intermittent exercise during uncompensable heat stress. *J. Appl. Physiol. In Press.*

21. Kuznetz, L. H. A two-dimensional transient mathematical model of human thermoregulation. *Am. J. Physiol. 237*: R266-R277, 1979.

22. Nadel, E. R., R. W. Bullard and J. A. J. Stolwijk. Importance of skin temperature in the regulation of sweating. *J. Appl. Physiol 31*: 80-87, 1971.

23. Roberts, M. F. and C. B. Wenger. Control of skin blood flow during exercise by thermal reflexes and baroreflexes. *J. Appl. Physiol.: Respirat. Environ. Exercise Physiol. 48*: 717-723, 1980.

24. Rowell, L. B., J. A. Murray, G. L. Brengelmann and K. K. Kraning, II. Human cardiovascular adjustments to rapid changes in skin temperature during exercise. *Circulation Res. 24*: 711-724, 1969.

25. Rowell, L. B. Cardiovascular adjustments to thermal stress. In: *Handbook of Physiology - The Cardiovascular System. Peripheral Circulation and Organ Blood Flow.* Bethesda, MD: Am. Physiol. Soc., 1983, sect. 2, vol III, part 2, chapt 27, p. 967-1023.

26. Rowell, L. B. (1986) *Human Circulation Regulation During Physical Stress.* New York, NY: Oxford, 1986.

27. Saltin, B. A., A. P. Gagge and J. A. J. Stolwijk. Muscle temperature during submaximal exercise in man. *J. Appl. Physiol 25*: 679-688, 1968.

28. Shitzer, A. (1975) Studies of bio-heat transfer in mammals. In: *Topics in Transport Phenomena.*, New York, NY: Halstead Press, J. Wiley, p. 211-243.

29. Sköldström, B. Physiological responses of fire fighters to workload and thermal stress. *Ergonomics 30*: 1589-1597, 1987.

30. Stolwijk, J. A. J. and J. D. Hardy. Temperature regulation in man - a theoretical study. *Pflugers Archiv. 291*: 129-162, 1966.

31. Stolwijk, J. A. J. and J. D. Hardy. Control of body temperature. In: *Handbook of Physiology. Reactions to Environmental Agents.* Bethesda, MD: Am. Physiol. Soc., 1977, sect.9, chapt. 4, p. 45-67.

32. Wissler, E. H. Mathematical simulation of human thermal behavior using whole body models. In: *Heat Transfer in Medicine and Biology. Analysis and Applications.* New York, NY: Plenum Press, 1985, vol. 1, chapt. 13, p. 325-373.

APPENDIX

RECENT ENHANCEMENT TO THE SIMULATION

A new feature has been added to the simulation since the initial preparation of this report. Since this is an addition to and not a change to the simulation as described in the main body of this report, it is treated as appendix material.

Hydration Status

The simulation now calculates changes in total body water. Initially, it is assumed that the subject is euhydrated. The size of the initial total body water compartment (TBW) is calculated as TBW = $0.72V_{nlat}$. This initial volume is simultaneously depleted by sweating an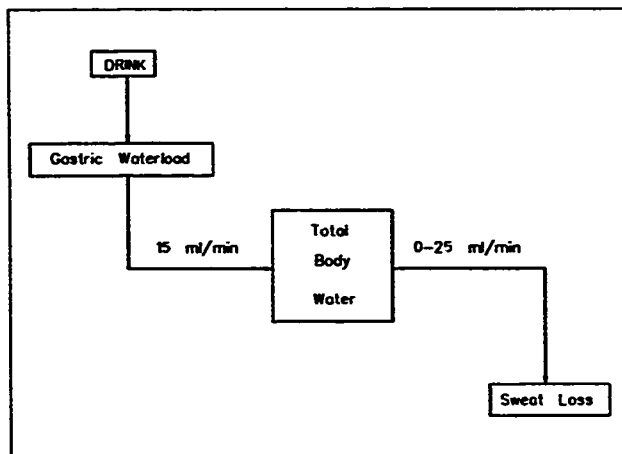d augmented by transport of water from the water-load compartment (Figure A1). The factor limiting the rate of transport from the water-load compartment into TBW is the rate of gastric emptying, not the rate of intestinal absorption., Gastric emptying rates of 15-20 ml•min^{-1} have been measured during exercise in the heat.

Figure A1. Illustration of algorithm for calculating the time course of change in total body water.

An example of a recent application of the simulation and, in particular, this new algorithm was as an aid in the design of a field investigation of soldiers' physiological responses to work in the desert at Ft. Bliss while wearing protective clothing. Part of the

39

protocol required soldiers to wear Battle Dress Undergarments and Battle Dress Overgarments in MOPP4 configuration while marching at 1.12 m·s⁻¹ with a 22 kg load for 24 minutes out of each 30 min period. Forty-five minutes prior to the march subjects were preloaded with 450 ml of water. The question arose: "Will subjects exceed the 5% limit on hydration before they exceed the upper rectal temperature limit of 39.5°C?"
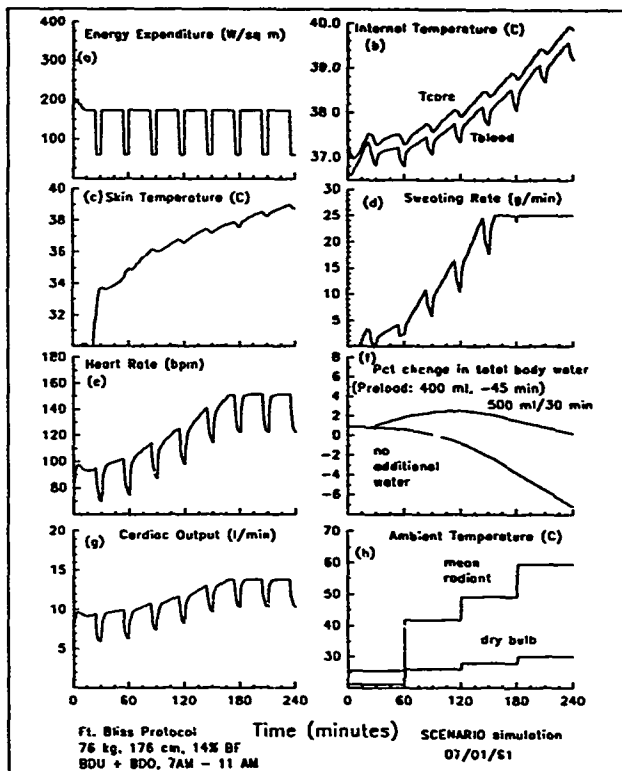

Figure 2A. Simulation of physiological responses to protocol of Ft. Bliss field study. Anticipated dry bulb and mean radiant temperatures were projected from other studies.

Two conditions were tested: (1) no further water and (2) 500 ml of water every 30 min. Panel (a) shows estimated energy expenditure while panel (h) shows estimated dry-bulb temperature and mean radiant temperature. These were estimated from typical temperatures in El Paso, TX during the month of July. The simulation results indicate that if the subjects drank no more water, the 5% dehydration limit and the 39.5°C limit on rectal temperature will occur at nearly the same time. On the other hand, if subjects drink 1 ℓ·hr⁻¹ one would anticipate hyper-hydration to the extent of 1-2% even when sweating at a maximal rate.

Glossary

A_D = Dubois surface area of subject [m^2 or cm^2]

A_{mp} = area of cylinder at midpoint between adjacent compartments [cm]

A_r = effective radiating area of the body surface [m^2]

BF_n = rate of blood flow through compartment n [$cm^3 \cdot min^{-1}$ or $\ell \cdot min^{-1}$]

C = rate of convective heat loss from skin surface [$W \cdot m^{-2}$]

C_{res} = rate of convective heat loss from respiratory tract [W or $W \cdot m^{-2}$]

CO = cardiac output [$cm^3 \cdot min^{-1}$ or $\ell \cdot min^{-1}$]

E = rate of evaporative heat loss from skin surface [$W \cdot m^{-2}$]

E_{max} = maximum rate of skin evaporative heat loss [$W \cdot m^{-2}$]

E_{res} = rate of evaporative heat loss from respiratory tract [W or $W \cdot m^{-2}$]

F'_{cl} = Burton's thermal efficiency factor for clothing, corrected [ND]

F'_{pcl} = Nishi's modified permeation efficiency factor for clothing [ND]

H = upright stature of subject [cm]

H_n = rate of heat production in compartment n [W]

HR = heart rate [$beats \cdot min^{-1}$]

I_{clo} = thermal insulation provided by clothing [clo]

K_{mn} = conductance between compartments m and n [$W \cdot °C^{-1}$]

L = cylinder height [cm]

M_{tot} = total rate of metabolic energy transformation [W or $W \cdot m^{-2}$]

$P_{s,sk}$ = vapor pressure of sweat on skin at temperature $\bar{T}_{sk}$ [Torr]

P_w = ambient water vapor pressure [Torr]

ΔQ_n = change in heat content of compartment n [$W \cdot min$]

R = rate of radiant heat loss from skin surface [$W \cdot m^{-2}$]

SV = cardiac stroke volume [ml]

T_a = ambient air (dry bulb) temperature [°C]

T_{cl} = clothing temperature [°C]

T_{es} = esophageal temperature [°C]

T_n = temperature of compartment n [°C]

T_o = ambient operative temperature [°C]

$\bar{T}_r$ = mean radiant temperature [°C]

T_{re} = rectal temperature [°C]

$\bar{T}_{sk}$ = mean weighted skin surface temperature [°C]

V = subject total body volume [cm³]

V_{cpmt} = volume of the *nth* annular compartment [cm³]

V_{fat} = subject body fat volume [cm³]

V_{nfat} = subject body non-fat volume [cm³]

V_{out} = volume, cylinder center to extent of the *nth* compartment [cm³]

$\dot{V}O_2$ = oxygen consumption [ℓ•min⁻¹]

$\dot{V}O_2max$ = maximal oxygen consumption [ℓ•min⁻¹]

W = subject body weight [kg]

W = rate of energy expenditure dissipated in external work [W or W•m⁻²]

c_n = heat capacity (specific heat) of compartment n [W•min•g⁻¹•°C⁻¹]

f_{cl} = Breckenridge clothing area factor [ND]

h = combined non-evaporative skin heat transfer coefficient [W•m⁻²•°C⁻¹]

h_c = convective heat transfer coefficient for skin [W•m⁻²•°C⁻¹]

h_e = evaporative heat transfer coefficient for skin [W•m⁻²•Torr⁻¹]

h_r = linear radiant heat transfer coefficient for skin [W•m⁻²•°C⁻¹]

i_m = Woodcock moisture index of water vapor through clothing [ND]

k_n = thermal conductivity of compartment n [W•cm•°C⁻¹•m⁻²]

$\dot{m}_{sw}$ = rate of sweat production [g•min⁻¹]

r = outside cylinder radius [cm]

r_{cm} = radius to the center of mass of the *nth* compartment [cm]

r_{in} = inner radius of the *nth* annular compartment [cm]

A_{mp} = area of cylinder at midpoint between adjacent compartments [cm]

r_{mp} = radius of cylinder at midpoint between adjacent compartments [cm]

t = time [minutes][1]

v_{air} = velocity of air movement on stationary subject [m•sec⁻¹]

v_{move} = velocity of subject movement in stationary air [m•sec⁻¹]

ℓ_{mn} = length of conduction path between compartments m and n.

ρ = subject average body density [g•cm⁻³]

ρ_{fat} = density of body fat components [g•cm⁻³]

ρ_n = average density of compartment n

---

[1]The simulation is constructed around the minute time base and, unless otherwise specified, values for variables and constants are in terms of minutes.

ρ_{nfat} = density of non-fat body components [$g \cdot cm^{-3}$]

σ = Stephan-Boltzman constant: $5.67 \cdot 10^{-8}$ [$W \cdot m^{-2} \cdot K^{-4}$]

λ = latent heat of sweat vaporization at T = 35°C [$W \cdot min \cdot g^{-1}$ or $J \cdot g^{-1}$]

$\%_{fat}$ = percent of subject body weight that is fat

DISTRIBUTION LIST

10 Copies to:

Commandant

Academy of Health Sciences

ATTN: HSHA-FR (USAMRDC Liaison Officer)

Fort Sam Houston, TX 78234-6100

4 Copies to:

Defense Technical Information Center

ATTN: DTIC-SDAC

Alexandria, VA 22304-6145

2 Copies to:

Commander

U.S. Army Medical Research and Development Command

ATTN: SGRD-OP

Fort Detrick

Frederick, MD 21702-5012

Commander

U.S. Army Medical Research and Development Command

ATTN: SGRD-PLE

Fort Detrick

Frederick, MD 21702-5012

Commander

U.S. Army Medical Research and Development Command

ATTN: SGRD-PLC

Fort Detrick

Frederick, MD 21702-5012

Commander
U.S. Army Medical Research Institute of Chemical Defense
Aberdeen Proving Ground, MD 21010-5425

Commander
U.S. Army Chemical Research, Development and Engineering Center
Aberdeen Proving Ground, MD 21010-5423

Commandant
U.S. Army Chemical School
Fort McClellan, AL 36205-5020

Commander
U.S. Air Force School of Aerospace Medicine
Brooks Air Force Base, TX 78235-5000

Commanding Officer
Naval Health Research Center
P.O. Box 85122
San Diego, CA 92138-9174

Director
U.S. Army Laboratory Command
Human Engineering Laboratory
ATTN: SLCHE-SS-TS
Aberdeen Proving Ground, MD 21005-5001

Commander
U.S. Army Biomedical Research and Development Laboratory
Fort Detrick
Frederick, MD 21702-5010

Commander
U.S. Army Medical Materiel Development Activity
Fort Detrick
Frederick, MD 21702-5009

Defence and Civil Institute of Environmental Medicine
ATTN: U.S. Army Scientific Liaison Officer
(U.S. Army Medical R&D Command)
1133 Sheppard Avenue W.
P.O. Box 2000
Downsview, Ontario
CANADA M3M 3B9

1 Copy to:

Commandant
Academy of Health Sciences, U.S. Army
ATTN: AHS-COM
Fort Sam Houston, TX 78234-6100

Stimson Library
Academy of Health Sciences, U.S. Army
ATTN: Chief Librarian
Bldg. 2840, Room 106
Fort Sam Houston, TX 78234-6100

Director, Biological Sciences Division
Office of Naval Research - Code 141
800 N. Quincy Street
Arlington, VA 22217

Commanding Officer

Naval Medical Research and Development Command

NMC-NMR/ Bldg. 1

Bethesda, MD 20814-5044

Office of Undersecretary of Defense for Acquisition

ATTN: Director, Defense Research and Engineering

    Deputy Undersecretary for Research & Advanced Technology

    (Environmental and Life Sciences)

    P   agon, Rm. 3D129

    Washington D.C. 20301-3100

Dean

School of Medicine

Uniformed Services University Of The Health Sciences

4301 Jones Bridge Road

Bethesda, MD 20814-4799

Commander

U.S. Army Aeromedical Research Laboratory

ATTN: SGRD-UAC

Fort Rucker, Alabama 36362-5292

Director

Walter Reed Army Institute of Research

ATTN: SGRD-UWZ-C (Director for Research Management)

Washington D.C. 20307-5100

Commander

U.S. Army Environmental Hygiene Agency

Aberdeen Proving Ground, MD 21010-5422

Commander
U.S. Army Military History Institute
Carlisle Barracks
ATTN: Chief, Historical Reference Branch
Carlisle, Pennsylvania 17013-5008

Commander
U.S. Army Natick Research, Development and Engineering Center
ATTN: STRNC-MIL
Technical Library Branch
Natick, MA 01760-5040

Commander
U.S. Army Natick Research, Development and Engineering Center
ATTN: STRNC-Z
Natick, MA 01760-5000

Commander
U.S. Army Natick Research, Development and Engineering Center
ATTN: STRNC-TAF
U.S. Air Force Liaison
Natick, MA 01760-5004

Commander
U.S. Army Natick Research, Development and Engineering Center
ATTN: STRNC-TAM
U.S. Marine Corps Liaison
Natick, MA 01760-5003

Commander
U.S. Army Natick Research, Development and Engineering Center
ATTN: STRNC-TAN
U.S. Navy Liaison
Natick, MA 01760-5003